Docket No. 50-213
B13388

Attachment

Haddam Neck Plant

Zircaloy Clad Fuel Mechanical Design Report

December 1989

NUSCO-166
November 1989

CONNECTICUT YANKEE ATOMIC POWER COMPANY
HADDAM NECK PLANT

Zircaloy Clad Fuel Mechanical Design Report

Northeast Utilities
P.O. Box 270
Hartford, Connecticut

TABLE OF CONTENTS

List of Tables

List of Figures

1.0 INTRODUCTION

This Topical Report provides the fuel mechanical design results for the Zircaloy clad fuel assembly to be used in the Haddam Neck Plant, Cycle 17 reload batch of fuel. Cycle 17 startup is currently planned for 1991. The conversion to Zircaloy cladding will achieve the goal of upgrading the fuel design to current industry standards and to provide greater fuel managment flexibility. The fuel mechanical design was performed by the current fuel supplier, the B&W Fuel Company. B&W has supplied stainless steel clad reload fuel for the Haddam Neck Plant since Cycle 7 (1976).

The Haddam Neck Plant has used stainless steel clad fuel since initial criticality in 1967, and is one of two remaining domestic stainless steel clad PWR cores. The cladding conversion program for the Haddam Neck Plant was initiated in 1981, with engineering feasibility studies. A Zircaloy clad, Lead Test Assembly (LTA) program was implemented for the startup of Cycle 13 in November 1984. Four Zircaloy clad fuel assemblies were designed and fabricated by B&W, with the goal of achieving three cycles of irradiation with Post Irradiation Examinations (PIEs) conducted at the end of each cycle. The four LTAs have completed the third cycle of use and had achieved an assembly average burnup of 35,000 MWd/mtU when discharged in September 1989.

The conversion of the Haddam Neck core to Zircaloy clad fuel will be accomplished on a batch basis (one-third of the core replaced each refueling) starting with Cycle 17 in 1991. Full conversion will be completed by the startup of Cycle 19 in 1994.

This Topical Report and the fuel mechanical results reported herein, will be validated on a cycle by cycle basis and will be the basis for the evaluation of future design changes. This document will be referenced in future reload licensing submittals, such as the Technical Report Supporting Cycle Operation.

2.0 SUMMARY

The fuel mechanical design goals that were established for the conversion effort include:

1. Use of approved B&W standard design methodology, following the guidelines provided in NUREG-0800, Section 4.2 and Appendix A.
2. Target fuel assembly design burnup of 50,000 MWd/mtU.
3. Minimize non-cladding design changes to maintain mechanical and thermal hydraulic compatability with the stainless steel clad fuel.
4. Apply the experience gained from the LTA program.

These design goals have been met with the fuel assembly mechanical design described herein. Section 3.0 provides a description of the design, and a comparison with the current stainless steel design and the LTA design. The results of the mechanical design analyses are provided in Section 4.0. Section 5.0 provides the results of the thermal hydraulic analyses and demonstrates the compatibility with the the stainless steel design.

3.0 FUEL ASSEMBLY DESIGN DESCRIPTION

3.1. Introduction

The Zircaloy fuel rod assembly (ZRFRA) is a 15x15 array fuel assembly with Inconel spacer grids, stainless steel top and bottom nozzles, instrument sheath and thimble tubes, and Zircaloy clad fuel rods. It was designed as a replacement assembly for the standard B&W Fuel Company (BWFC) Haddam Neck assembly which uses stainless steel for the fuel rod cladding. A comparison of the two designs is shown in Figure 3-1. The fuel rod design was developed with standard BWFC methods. The design maintains the same fuel rod outside diameter to maintain hydraulic compatibility and includes many of the design features of the Lead Test Assemblies (LTAs). Table 3-1 provides a comparison of the ZRFRA physical parameters to those of the LTA and stainless steel clad fuel assemblies.

Section 3.2 provides a summary of the features that are common to the ZRFRA and stainless steel designs. Section 3.3 summarizes the features that are unique to the ZRFRA.

3.2. Standard Design Features

The fuel assembly consists of 204 fuel rods, 20 thimble tubes, and one instrument sheath in a 15x15 square array. The thimble tubes provide guidance for control rod insertion and are attached to the top and bottom nozzles and welded to the Inconel spacer grids along the fuel assembly to form the structural skeleton. A reduced diameter section at the bottom of the thimble tubes decelerates the control rod assemblies during a reactor trip. The instrument sheath occupies the center lattice position and provides guidance and protection for the incore instrumentation assemblies. The top nozzle assembly contains the fuel assembly holddown springs and is attached to the thimble tubes by removable nuts and locking cups. The bottom nozzle is attached to the thimble tubes by locking nuts which are mechanically captured by crimping. The fuel rod and thimble tube spacing is maintained along the length of the fuel assembly by seven Inconel spacer grids.

The top nozzle and the holddown leaf springs for the two designs are identical. The Inconel spacer grids and the way that they are attached to the thimble tubes are identical for both designs. The mechanisms for attaching the top and bottom nozzles are also identical.

3.3. Unique Design Features

The fuel rod design consists of cylindrical ceramic UO_2 pellets contained in a Zircaloy-4 tube with end caps welded at each end. A single plenum spring at the top end and tubular spacers at both ends position the fuel stack within the cladding and provide protection against axial gap formation during shipping and handling. The fuel rod is evacuated and then backfilled with helium of high purity at high pressure prior to seal welding. The high purity helium assures good heat transfer across the pellet-cladding gap. In addition the high pressure fill gas prevents creep collapse of the fuel rod during the expected incore operation of the fuel rod. A comparison of the stainless steel, LTA, and Zircaloy fuel rod designs is provided in Figure 3-2.

The ZRFRA bottom nozzle is shorter than the bottom nozzle on the stainless steel clad fuel assembly. The legs on the bottom nozzle have been shortened, and the thimble tube reduced diameter sections and the instrument sheath have been lengthened on the ZRFRA to maintain the same overall assembly height as the stainless steel fuel assemblies. The axial spacer grid elevations are slightly different on the ZRFRA design to minimize the effects of mechanical and thermal-hydraulic interaction between fuel assemblies. The top and bottom spacer grids are shifted to positions slightly inboard of the locations of the corresponding spacer grids on stainless steel fuel assemblies. The five intermediate spacer grids are located at the same elevations on both types of assemblies.

Table 3-1. Fuel Assembly Parameter Comparison

	Stainless Steel	LTA	ZRFRA
Fuel Rod Array	15x15	15x15	15x15
Cladding Material	304SS	Zirc-4	Zirc-4
Fuel Rods per Assembly	204	204	204
Rod Pitch, inches	0.563	0.563	0.563
Fill Gas Pressure, psia	54.7	279.7	279.7
Fuel Rod Length, inches	126.68	126.125	125.875
Fuel Stack Length, inches	120.5	119.0	118.575
Fuel Rod O.D., inches	0.422	0.422	0.422
Cladding Thickness, inches	0.0165	0.027	0.027
Diametral Gap, inches	0.0065	0.007	0.007
Fuel Pellet Diameter, inches	0.3825	0.361	0.361
Fuel Pellet Length, inches	0.458	0.425	0.425
Fuel Density, % theoretical	95	95	95

Figure 3-1. Design Comparison

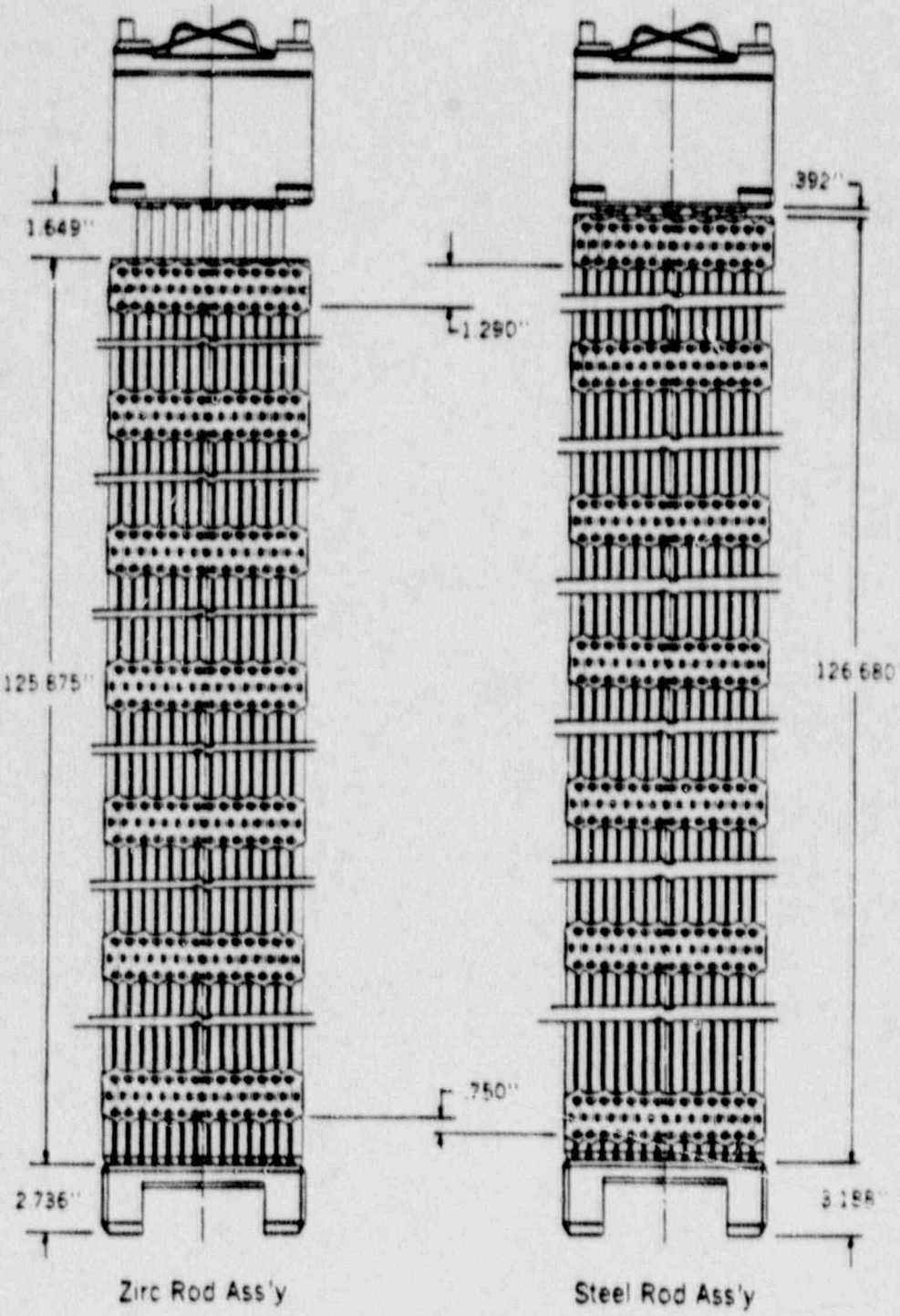

Figure 3-2. Haddam Neck Fuel Rod Design

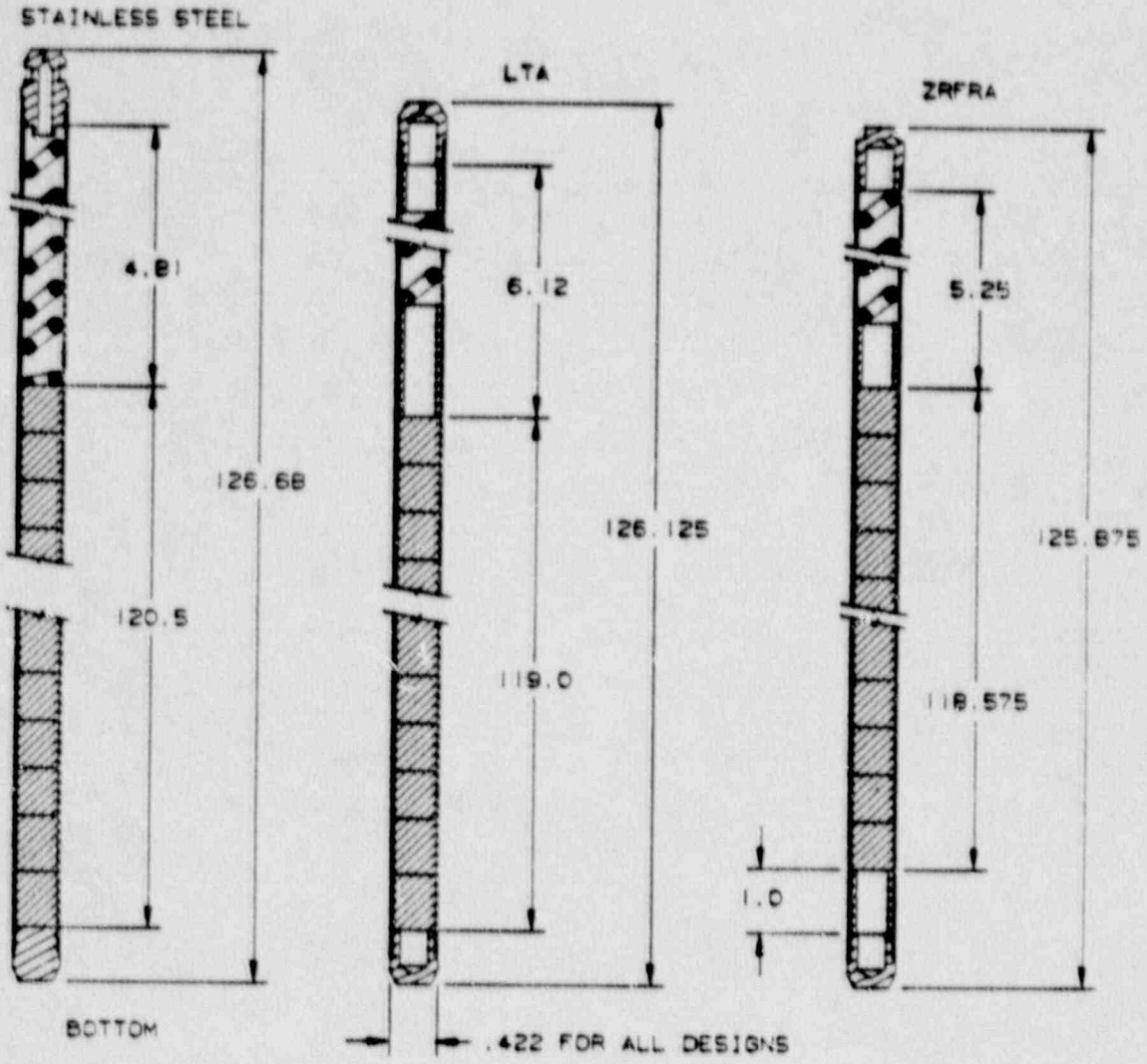

4.0 MECHANICAL DESIGN ANALYSIS

4.1 Introduction

The Zircaloy fuel rod fuel assembly (ZRFRA) and fuel rod mechanical design are analyzed for performance using standard BWFC methods for the following four plant conditions:

Condition I -	Normal Operation
Condition II -	Incidents of moderate frequency (upset conditions)
Condition III -	Infrequent incidents (emergency conditions)
Condition IV -	Limiting faults (faulted conditions)

Margins: Margins are calculated by the following:

Margin % = [(Allowable - Predicted)/Predicted] * 100 %

The method of analysis for each criteria and the inputs used are conservative. A margin of > 0 % is sufficient. References for the analysis methods are provided where appropriate in the text of each section.

The static and dynamic structural characteristics of the ZRFRA have been determined analytically and experimentally and were found to be compatible with the stainless steel clad resident fuel assemblies. The ZRFRAs have been designed to maintain their mechanical design integrity through 4 cycles of operation, with a maximum assembly burnup of 50,000 MWd/mtU.

The following discussion addresses the analyses used to verify the structural adequacy of the ZRFRAs for design loadings and the evaluation of mechanical compatibility of the ZRFRA and the stainless steel clad resident fuel assemblies.

4.2 Fuel Rod Design Evaluation

A series of analyses were performed on the ZRFRA fuel rod design to assure that its mechanical performance in-reactor would be in compliance with the acceptance criteria specified in Section 4.2 and Appendix A of NUREG-0800 (Reference 1). The areas analyzed are:

a. Cladding Stress
b. Cladding Strain
c. Cladding Fatigue
d. Creep Collapse
e. Fuel rod growth
f. Shipping and handling

Items e and f are discussed in the fuel assembly design evaluation Section 4.3. Items a through ds are discussed in the following:

4.2.1 Fuel Rod Cladding Stress

Criteria: Cladding stress levels must be less than certain limits. Limits are based on ASME criteria. Stress level intensities are calculated in accordance with the ASME Code, which includes both normal and shear stress effects. These stress intensities are compared to Sm. Sm is equal to 2/3 of the minimum specified unirradiated yield strength of the material at the operating temperature (650 deg F). The limits are as follows:

Primary general membrane stress intensities (Pm) must not exceed Sm.

Local primary membrane stress intensities (Pl) must not exceed 1.5 * Sm. (These include the contact stresses from spacer grid hard stop-fuel rod contact.)

Primary membrane + Bending stress intensities (Pl +Pb) must not exceed 1.5 * Sm.

Primary membrane + Bending + Secondary stress intensities (Pl+Pb+Q) must not exceed 3.0 * Sm.

The fuel rod stresses under faulted conditions are evaluated using primarily the methods outlined in Appendix F of the ASME Boiler and Pressure Vessel

Code, Section III. (Reference 2)

Stress intensity calculations combine the stresses so that the stress intensity is maximized.

Classifications of Stresses:

Loading Condition	Stress Category
Pressure Stresses	Pm
Ovality Stresses	Pb
Spacer Grid Interaction	Pl
Flow Induced Vibration	Pb
Radial Thermal Expansion	Q
Differential Rod Growth	Q

Pressure and temperature inputs to the stress intensity analyses are chosen so that the operating conditions for all Condition II transients are enveloped.

Results: The fuel rod cladding was analyzed for the stresses induced during operation. The ASME pressure vessel stress intensity limits were used as guidelines. Conservative values were used for cladding thickness, oxide layer buildup, external pressure, internal fuel rod pressure, differential temperature and unirradiated cladding yield strength. The analysis results show that the maximum cladding stress intensities are within limits under all loading conditions.

Loading Condition	Stress Intensity Limit	Minimum Margin %
Primary Membrane	Sm	41
Primary Membrane + Bending	1.5 Sm	90
Primary Membrane + Bending + Secondary	3.0 Sm	108

4.2.2 Fuel Rod Cladding Strain

Criteria: The uniform transient strain (elastic and inelastic) shall not exceed 1%. This is defined as the transient induced deformation with gage lengths corresponding to the

cladding dimensions. The transient strain is calculated from the change in diameter of the fuel pellet during the maximum power transient the fuel rod is expected to undergo. This is done as the maximum strain would occur at the cladding inside diameter, and the cladding deformation is driven by the fuel pellet expansion.

The transient strain shall be determined using the computer code TACO2 described in Reference 3.

Results: The fuel rod was analyzed to determine the maximum power transient the fuel rod could experience before the transient strain limit of 1% was exceeded. The transient strain limit uses cladding circumference changes before and after a linear heat rate (LHR) transient to determine the strain. The transient required to exceed this limit was found to be 19.88 Kw/ft, which is much greater than the maximum transient the fuel rod is expected to experience.

4.2.3 Fuel Rod Cladding Fatigue

Criteria: The total fatigue usage factor for all condition I and II events shall not exceed 0.9. The fatigue curve from Reference 4 shall be used.

Results: The fuel rod was analyzed for the total fatigue usage factor using the ASME pressure vessel code as a guideline. A fuel rod life of 6 years is assumed. All possible condition I & II events expected and one condition III event are analyzed to determine the total fatigue usage factor experienced by the fuel rod cladding. Conservative inputs in terms of cladding thickness, oxide layer buildup, external pressure, internal fuel rod pressure and differential temperature across the cladding are assumed. The results of the fatigue analysis show a maximum fatigue usage factor of .48 which is less than the maximum allowable of 0.9.

4.2.4 Fuel Rod Cladding Creep Collapse

Criteria: Creep collapse of the cladding due to creep ovalization will not be predicted during the incore life of the fuel rod.

Results: Creep collapse life of BWFC fuel rod designs has previously been determined with the computer code CROV which is described in Reference 5. CROV uses manufacturing data to provide the cladding dimensional inputs, and TACO2 (Reference 3) to provide the temperature, the pressure, and the fast neutron flux level history inputs for the fuel rods. Using CROV, a creep collapse life for the ZRFRA fuel rods was determined

to be at a burnup of > 50,000 MWd/mtU based on a bounding power history.

The creep collapse life prediction from CROV is based on an axial gap of greater than 0.5 inches length forming at a high flux portion of the fuel rod. Experience with high burnup fuel rods show that axial gaps in modern high density (95 % T.D.) fuel stacks are rare and less than 0.1 inches in length (Reference 6). Even fuel rods with lower density fuel (92.5% T.D.) showed a maximum gap of 0.3 inches (Reference 6). Based on this experience no creep collapse is anticipated nor will analysis be performed on the fuel rods of a batch as long as an envelope of operating and manufacturing parameters is maintained. This method has been previously approved for the Mark-B fuel rod design which is similar to the ZRFRA fuel rod design (Reference 7). The envelope is:

	Parameter	Nominal Value	Limit
Cladding:	Wall Thickness	27.0 mils	26.0 mils, LTL ($x - 2\sigma$)
	Initial Ovality	0.7 mils	1.0 mils, UTL ($x + 2\sigma$)
Prepressure:		265 psig	> 260 psia, LTL
Fuel Pellet:	Density	95.0% T.D.	94.8% T.D., LTL
	Individual Pellet Resinter Density, $\Delta\rho$	1.5% T.D.	2.5% T.D., UTL
Burnup:			<55,000 MWd/mtU, max

Individual pellet resinter density is based on the maximum allowable in the fuel pellet specification and is process qualified.

4.3 Structural Integrity Evaluation.

The requirements that must be met to insure the structural integrity of the fuel assembly, and the results of analyses to determine if those conditions are met, are presented in this section. The structural integrity under normal operation is discussed first. The integrity of the fuel assembly under the accident conditions of seismic and LOCA events is then presented. The criteria that must be meet for both normal and accident conditions are listed below.

Stress Criteria: The stress intensities in the upper and lower nozzles (excluding the holddown spring), the thimble tubes, and the fuel rods (condition IV only) shall be less than

the following limits. All stress nomenclature is per ASME Boiler and Pressure Vessel Code, Section III. (Reference 2)

Condition	Stress Intensity Limit
Condition I & II	$P_m \leq 1.0\ S_m$
(normal operation	$P_l \leq 1.5\ S_m$
& upset condition)	$P_m + P_b \leq 1.5\ S_m$
	$P_m + P_b + Q \leq 3.0\ S_m$
Condition IV	$P_m \leq 2.4\ S_m$ or $.7\ S_u$
(faulted condition)	$P_m + P_b \leq 3.6\ S_m$ or $1.05\ S_u$ whichever is less

where

P_m = general primary membrane stress intensity

P_l = local primary membrane stress intensity

P_b = primary bending stress intensity

Q = secondary stress

S_m = allowable membrane stress intensity:

= 2/3 Sy or 1/3 Su, whichever is less at room temperature, or 1/3 Su or .9 Sy at operating temperature, but not to exceed 2/3 of the minimum specified yield strength at room temperature. These are unirradiated material properties.

S_y = minimum yield stress

S_u = ultimate stress

Criteria for buckling of thimble tubes: Thimble tube buckling shall not occur during normal operation (Condition I) or any transient condition where control rod insertion is required by the safety analysis.

Results: Calculations show that the thimble tubes will not buckle under the maximum loads calculated.

4.3.1 Normal Operation

4.3.1.1 Fuel Rod Fretting

Criteria for fretting: The fuel assembly design shall be shown to provide sufficient support

to limit fuel rod vibration and clad fretting wear.

Results: Fuel rod fretting performance is based on Post Irradiation Examination (PIE) data from B&W fuel assemblies. Examination of standard Inconel spacer grid MK-B fuel rods at 50.2 GWd/mtU, and Zircaloy intermediate spacer grids at 38 GWd/mtU show no sign of fretting wear (References 8 and 9). The MK-B Inconel and Zircaloy spacer grids bound the ZRFRA spacer grid grip force at the higher and lower bound. In addition, examination of stainless steel clad fuel rods from Haddam Neck during fuel assembly reconstitution also showed no signs of fretting wear.

4.3.1.2 Fuel Rod Bowing

Criteria for Fuel Rod Bowing: Fuel rod bowing shall be evaluated with respect to the mechanical and thermal/hydraulic performance of the fuel assembly. The fuel assembly shall not exhibit excessive fuel assembly bow during its operation life.

Results: PIE results of the LTAs indicate the magnitude of fuel rod bow is similar to other BWFC Zircaloy clad fuel assembly designs such as the Mark-B, Mark-BZ and Mark-C. This similarity justifies the application of the fuel rod bow prediction correlation for water channel closure presented in the B&W fuel rod bow topical report (Reference 10). The report concludes there is an insignificant DNBR impact caused by water channel closure.

4.3.1.3 Fuel Rod Growth Gap

Criteria: The fuel assembly to reactor internals gap allowance and upper nozzle to fuel rod growth gap allowance shall be designed to provide a positive clearance during the assembly life time.

Results: The axial gaps between the top nozzle and reactor core plates and between the top nozzle and fuel rod conservatively allow sufficient margin to accommodate the fuel assembly and fuel rod growth. PIE measurements on stainless steel clad fuel assemblies and on the LTAs show that the stainless steel thimble tubes undergo no irradiation growth. The irradiation growth of the fuel rods was conservatively based on EPRI and B&W PIE data, including the LTAs. The shoulder gap margin is sufficient to permit fuel assembly burnups of 50,000 MWd/mtU.

4.3.1.4 Fuel Assembly Holddown Springs

Criteria: The holddown spring system shall be capable of maintaining fuel assembly contact with the lower support plate during Condition I & II events. The fuel assembly top and

bottom nozzles shall maintain engagement with reactor internals for all Condition I-IV events. The fuel assembly shall not compress the holddown spring to solid height for any Condition I or II event.

Results: The holddown springs are designed to accommodate the differential thermal expansion between the fuel assembly and the core internals and irradiation growth. The fuel assembly holddown springs provide adequate holddown capability to keep the fuel assemblies in contact with the lower core plate throughout the design life during all Condition I and II events. The holddown springs are designed to tolerate the possibility of a deflection associated with a fuel assembly lift off and provide contact between the fuel assembly and the lower core plate. The top nozzle provides positive retention of the holddown spring in case of the very unlikely event of spring breakage.

The holddown force of the springs was verified by assembling springs into a top nozzle, and then obtaining a force versus deflection curve from compression testing of the holddown spring assembly. The force deflection curve was then used in an analysis to determine the results reported here.

4.3.1.5 Fuel Assembly Spacer Grids

Criteria for spacer grids: No crushing deformation of the spacer grids shall occur due to normal operation (Condition I) and Condition II event loading, and that the spacer grids provide adequate support to maintain the fuel rods in a coolable configuration for all conditions.

Results: No crushing deformation of the spacer grids will occur during condition I and II events.

4.3.2 Seismic and LOCA

Criteria: The following criteria have been established for the fuel assembly seismic analysis which are consistent with the acceptance criteria of the Standard Review Plan (NUREG-0800). Section 4.2. (Reference 1)

1) For operational basis earthquake (OBE) the fuel assembly is designed to ensure safe operation following an OBE.

2) For safe shutdown earthquake (SSE) the fuel assembly is designed to allow control rod insertion and to maintain a coolable geometry.

3) For loss of coolant accident (LOCA) or combined LOCA plus SSE the fuel assembly is designed to allow for the safe shutdown of the reactor systems.

4.3.2.1 Fuel Assembly Structural Integrity

Results: The fuel assembly response resulting from seismic and LOCA loads was verified as acceptable using the methodology given in BAW-10133P (Reference 11). This report has received the NRC approval for referencing in licensing applications. It was shown that the fuel assembly mechanical integrity is maintained and thus a coolable geometry is assured during all the seismic and LOCA loads postulated for the Haddam Neck reactor.

Although the skeleton design of the ZRFRA has minimal changes over the stainless steel design to give maximum compatibility, some ex-reactor testing was performed to support the seismic and LOCA analyses. The first test, which was performed at the Alliance Research Center (ARC), was a spacer grid impact test. This test determined the loads required to deform the spacer grids and was used in the horizonal LOCA and seismic analyses. The second test was performed at the Commercial Nuclear Fuel Plant (CNFP). In that test the frequency and damping characteristics of the Haddam Neck stainless steel clad fuel assembly were determined. The differences between the ZRFRA and the stainless steel clad fuel assembly have been shown by analysis to be slight. These testing data were used in the analyses which are further discussed in the following sections.

4.3.2.2 Fuel Assembly Seismic Analysis

The time history motions of the upper and lower core grid plates and at the upper core plate were obtained from the reactor system seismic analysis for the Haddam Neck Reactor. These motions were applied to the core model as shown in Figure 4-1. The maximum grid impact forces obtained from the seismic analysis are within the allowable limits as determined by the spacer grid impact tests described previously.

4.3.2.3 Fuel Assembly LOCA Analysis

The design basis LOCA assumed for the fuel assembly analysis was the leak before break LOCA event. The fuel assembly response resulting from the design case pipe break (a 10 inch diameter surge line break or a 10 inch diameter residual heat removal (RHR) line break) was analyzed using the core model shown in Figure 4-1 to determine the grid impact forces and deflections. The time history motions resulting from the LOCA breaks were obtained from a structural LOCA analysis of the reactor coolant system. The loads for LOCA plus SSE were combined by the square root of the squares method as discussed and accepted by

the NRC in Reference 1, NUREG-0800, the Standard Review Plan. The grid impact forces are well within the allowable limits as determined by the spacer grid impact tests.

4.3.2.4 Vertical LOCA Analysis

Separate models of the fuel assembly were derived for the vertical and horizonal directions. A schematic of the vertical assembly model is given in Figure 4-2. The methods outlined were applied to both models. Only the LOCA cases were evaluated in the vertical direction, as the upper and lower grid plates move in phase for the seismic case and cause no fuel assembly loading.

The maximum loads from the vertical and horizonal cases are superimposed by the square root sum of the squares method. The resultant loads were evaluated at critical component locations, the mechanical integrity of which was then evaluated. All components showed high margins of safety.

4.3.2.5 Standard Review Plan 4.2 Appendix A Analysis

The analyses required by Appendix A of NUREG-0800, Revision 2 were performed. Specific analyses performed included 1) performance of a "sample problem" designed to exercise various features of the code used in the analysis and reveal their behavior; 2) performance of a model sensitivity analysis utilizing +/- 10% variations in input amplitude and frequency; and 3) the addition of 30% loads to normal calculated LOCA loads to account for a pressure pulse which is associated with steam flashing.

All analyses showed full compliance with the requirements of the Standard Review Plan 4.2 Appendix A.

4.3.2.6 Mixed Core Analysis

A mixed core bounding analysis of seismic and LOCA events was performed for ZRFRAs and stainless steel clad fuel assemblies representative of transition cores. The results of the analysis were compared with the faulted conditions analysis results of the ZRFRA full core configuration. The resulting change in spacer grid impact loads are minor (within 3%). The spacer grid impact loads are well within the elastic load limit, and hence the requirement of a core coolable geometry is met.

4.4 Handling Characteristics

4.4.1 Shipping and Handling

The ZRFRA is designed to maintain its dimensional and structural integrity when subjected to normal shipping and handling loads. To preclude spacer grid crushing failures resulting from excessive clamping loads imposed by the shipping container, BWFC has developed a mechanical bracket that mechanically limits the imposed load. This configuration has been used to successfully ship over 500 Haddam Neck fuel assemblies.

Fuel assembly shipping criteria: The spacer grids will maintain sufficient grip on the fuel rods to prevent axial movement during shipping and handling at axial loads of up to 4g. Lateral loads of up to 6g will not cause setting of spacer grid spring stops.

Fuel rod shipping criteria: The plenum spring-spacer system must prevent gap formation in the fuel stack during transport up to an axial loading of 4g.

Results:

1. The plenum spring is designed to maintain the fuel column position and prevent the formation of axial gaps. This is done by maintaining a preload on the fuel stack to counter acceleration loads which can occur during shipping and handling. The fuel assembly is very unlikely to experience the maximum axial shipping acceleration of 4g used in the analysis. In the unlikely event of a 4g acceleration the fuel stack position and the preload will be maintained.

2. The fuel rod will not slip through the spacer grids under the maximum axial shipping loads.

3. The spacer grids will maintain their structural integrity under the maximum lateral shipping loads, and under the maximum clamping loads of 600 lbs.

4. Spacer grid soft stops are designed to maintain acceptable fuel rod grip forces under the most adverse lateral shipping loads. The 6g lateral acceleration used in the analysis is also very conservative with respect to actual shipping conditions.

4.4.2 Bow and Twist

Fuel assembly bow and twist criteria: The bow and twist of the fuel assembly must be

limited to prevent problems with the handling equipment.

Results: Excessive fuel assembly bow and twist is not a problem due to the use of stainless steel thimble tubes. PIE measurements show no irradiation growth of the thimble tubes. No significant handling problems have been encountered after two cycles of operation for the LTA, or four cycles of operation for the stainless steel clad design.

4.4.3 Mechanical Design Compatibility Evaluation

The ZRFRA design data are provided in Table 3-1. In this table, comparisons are made between the current stainless steel clad fuel assembly, the LTA and the ZRFRA to show design similarities and differences. Figure 3-1 shows a ZRFRA full length schematic view along with the current stainless steel clad fuel assembly. The ZRFRA has the same cross-sectional envelope as the current stainless steel clad fuel assembly. Mechanical interaction between fuel assemblies is confined to the spacer grid locations. The spacer grid elevations of the ZRFRA match or overlap the current stainless steel clad fuel assembly, minimizing the effects of mechanical and hydraulic interaction between assemblies. The ZRFRA is designed to be fully compatible with the current stainless steel clad fuel assembly design, reactor internal interfaces, fuel handling and refueling equipment, and new and spent fuel storage racks. Compatibility of the existing control components with the ZRFRA design is assured by the similarity of critical dimensions such as thimble tube locations with those used in the current stainless steel clad design.

4.5 Material Compatibility

Criteria: The materials used in the manufacture of the fuel assembly and the fuel rod must be compatible with all other materials in the primary system. The fuel rod must be able to meet all criteria with the maximum expected oxide thickness present on the inside and outside of the cladding for the condition analyzed.

Results: The materials used in the ZRFRA were reviewed for compatibility with the primary water chemistry in use in the Haddam Neck reactor. Items that were checked were the expected oxidation rate of Zircaloy-4 cladding, caustic stress corrosion cracking from high lithium levels, and stress corrosion cracking of Inconel alloys used in the holddown springs and spacer grids. The primary chemistry limits for the Haddam Neck Reactor were also compared to those given for B&W 15x15 plants in Reference 12. Conformance with the guidelines in Reference 13 was also checked. The chemistry limits for the Haddam Neck reactor were the same or were enveloped by those from Reference 12. All of the materials used in the ZRFRA have been used in conjunction with each other in B&W MK-B fuel

assemblies. The experience of this use is applicable to the ZRFRA. For instance, the maximum oxide thickness used in the Section 4.2 analysis is based on MK-B poolside PIE and hotcell examination. PIE work on the LTAs showed no indication of adverse material reactions with the primary coolant.

4.6 Operational Experience

BWFC experience with reload fuel for the Haddam Neck reactor started with the manufacture of fuel assemblies for Cycle 7. As of June 1989 a total of 476 BWFC manufactured fuel assemblies, including four LTAs with Zircaloy-4 clad fuel rods have been irradiated at Haddam Neck.

4.6.1 Zircaloy-4 Clad Fuel

In order to verify the operation of a Zircaloy clad fuel rod design, four LTAs with Zircaloy-4 clad rods were irradiated in the Haddam Neck reactor. The design of the LTA fuel rod is shown in Table 3-1. Irradiation of the LTAs started with Cycle 13. Following Cycles 13 and 14 a poolside post irradiation examination was performed on the LTAs. Items that were checked were fuel rod growth, fuel rod bow, fuel assembly growth and bow, and general fuel assembly condition. After the second cycle of exposure an ultrasonic examination for leaking fuel rods was performed on all fuel assemblies from Cycle 14. No leaking fuel rods were found in the LTAs, with a burnup of 23,589 MWd/mtU after two cycles of exposure. A PIE was conducted after Cycle 15 when the LTAs were discharged with a burnup of 35,000 MWd/mtU. They were found to be sound and no anomalies were noted.

4.6.2 Stainless Steel Clad Fuel

The remaining 472 fuel assemblies produced by BWFC for Haddam Neck were of the stainless steel clad design. The stainless steel clad fuel design has achieved a maximum rod burnup of 39,200 MWd/mtU and an in-core exposure of four cycles. The mean average burnup of stainless steel fuel rods discharged in 1987 was 33,800 MWd/mtU. These fuel assemblies have performed well. Examination of fuel rods removed when a stainless steel clad fuel assembly was recaged showed that the fuel rods were in good condition with no wear at spacer grid contact sites.

Figure 4-1. Horizontal Core Seismic Model

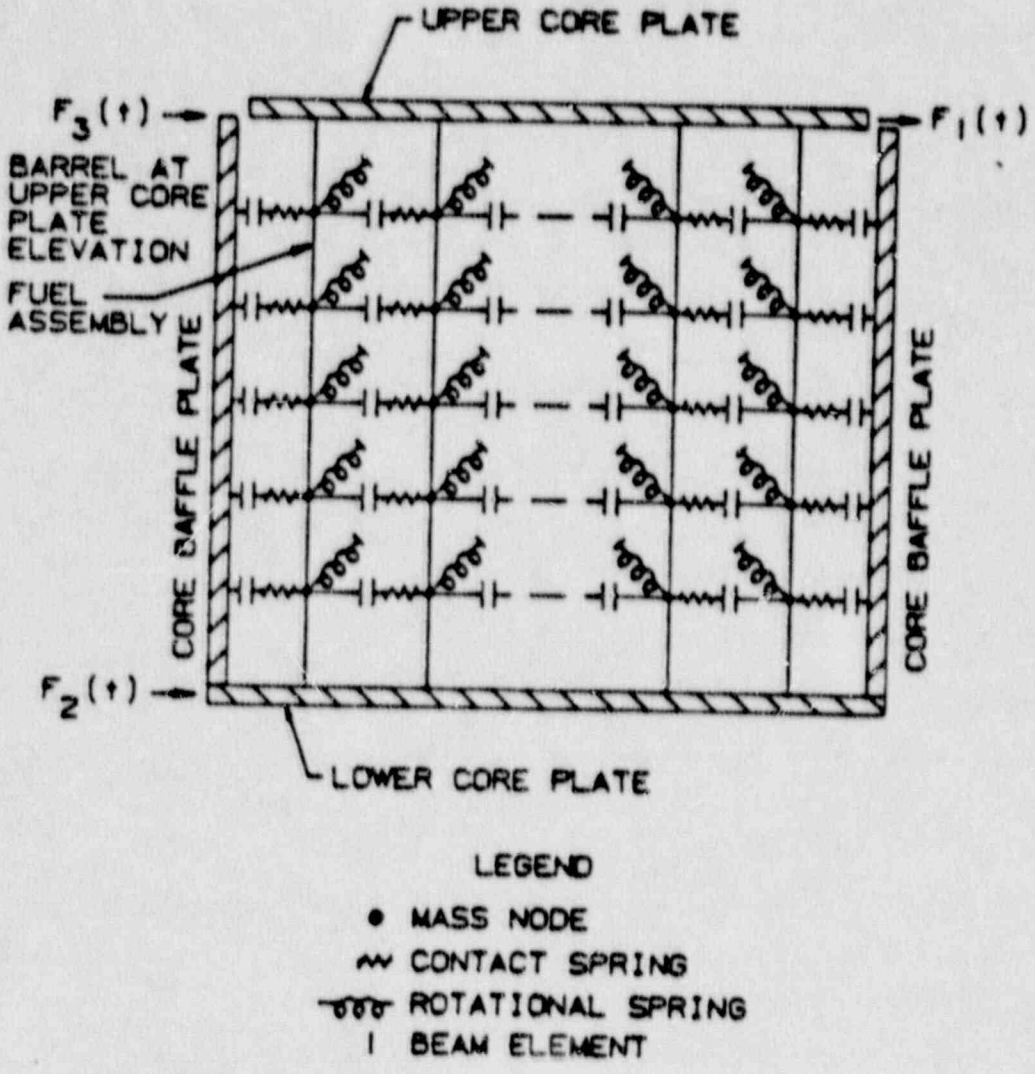

Figure 4-2. Fuel Assembly Vertical LOCA Model

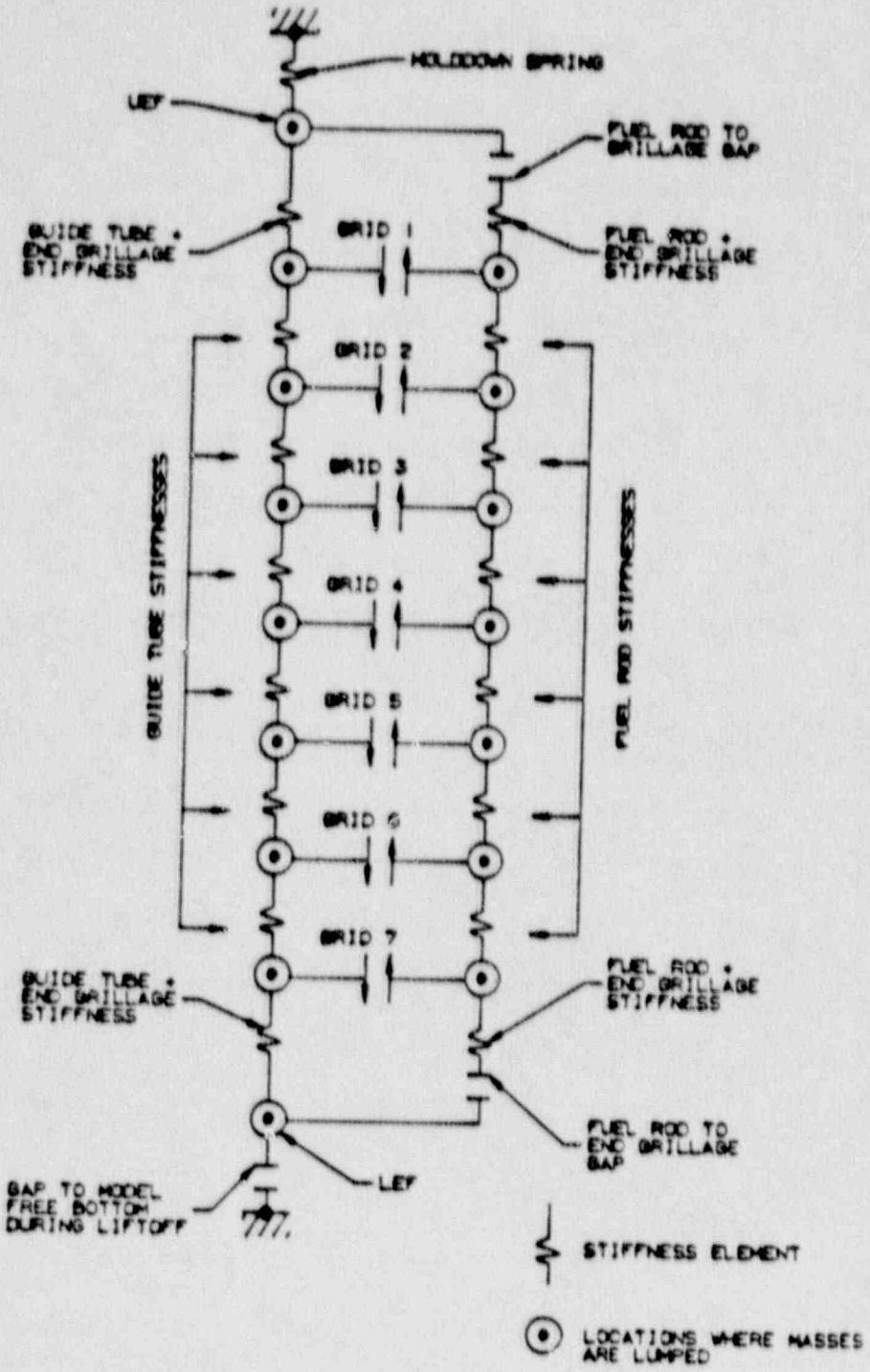

5.0 THERMAL HYDRAULIC DESIGN EVALUATION

5.1. Introduction

The Zircaloy fuel rod assembly (ZRFRA) design is hydraulically similar to the resident stainless steel clad fuel assembly design. The following discussions pertaining to the hydraulic, Departure from Nuclear Boiling (DNB), and fuel rod performance of the ZRFRA design are based on the assumption of a full reactor core of the ZRFRA fuel assembly design. The thermal hydraulic consequences of a mixed core where stainless steel clad and Zircaloy clad fuel assembly designs both reside in the core are discussed in Section 5.5 Transition Cycles.

Thermal hydraulic analyses have been performed to support the design of the ZRFRA. These analyses utilized two computer codes. The LYNX1 code, Reference 14, was used to determine the pressure drop effects of the new fuel design. The TACO2 code, Reference 3, was used to determine the in-reactor fuel performance for the Zircaloy clad fuel rod. The relative DNBR performance of the ZRFRA design was evaluated and found to be acceptable.

5.2. Hydraulic Performance

The Zircaloy clad fuel assembly was designed to be hydraulically compatible with the resident stainless steel clad fuel. The most noteworthy differences between the two designs that could affect the hydraulic performance of the designs are as follows:

a) The height of the ZRFRA bottom nozzle legs is less than that of the stainless steel design (see Figure 5-1). This has an insignificant effect on pressure drop and consequently on hydraulic performance.

b) The ZRFRA end grids are slightly more "inboard" within the fuel assembly than for the stainless steel design (see Figures 5-2 and 5-3), resulting in slightly different axial positions for the end grids. This difference also has an insignificant effect on pressure drop and consequently on hydraulic performance.

c) The vertical gap between the top of the fuel rods and the bottom of the top nozzle is larger for the ZRFRA design than for the stainless steel design (see Figure 5-3). This has a very small effect on pressure drop.

When the ZRFRA and stainless steel designs are compared, it is apparent that the flow

streams through the active fuel region of the fuel assemblies are essentially identical due to the common subchannel geometry and spacer grid design. The axial locations of all spacer grids in the active fuel region with the exception of the bottom spacer grid are common between the designs as shown in Figure 3-1. Therefore, the hydraulic resistances in the primary region of the core are the same for the two designs. The slight hydraulic differences between the ZRFRA and stainless steel designs are caused by the fuel assembly component arrangements below and above the fuel assembly active fuel region.

In order to accommodate the anticipated Zircaloy irradiation growth, the bottom nozzle for the ZRFRA design is shorter than the bottom nozzle for the stainless steel design as shown in Figure 5-1. Since the hydraulic resistance of the bottom nozzle is a result of the flow area change through the nozzle grillage (contraction/expansion) and the frictional surfaces, and the grillages are identical for the ZRFRA and stainless steel designs, the pressure drop from the bottom of the bottom nozzles to a common axial location above the nozzles will be virtually identical.

During power operation, the stainless steel clad fuel rods remain seated on the bottom nozzle as positioned during fuel assembly fabrication. However, the Zircaloy fuel rods are raised above the top of the bottom nozzle during power operation as a result of the different thermal expansion characteristics of the Zircaloy clad fuel rods and the stainless steel fuel assembly structure. The gap occurring between the fuel rods and the top of the bottom nozzle reaches a maximum following the plant startup from cold conditions and begins to decrease as a result of the irradiation-induced Zircaloy fuel rod growth. The gap below the fuel rods introduces a flow area change not present in the stainless steel design. The pressure drop effect of the gap results in a 1 percent higher pressure drop for the ZRFRA design over the stainless steel design at beginning of cycle (BOC) which will decrease with fuel exposure and will eventually disappear when the fuel rods make contact once again with the bottom nozzle.

Inside the bottom nozzle of the ZRFRA design, a bullet-nosed recess has been incorporated into the grillage to allow clearance for the fuel assembly locating pins (see Figure 5-1). The recess was necessary to permit a bottom nozzle with shorter legs. The projection of the locating pin into the plane of the grillage will have an insignificant effect on the pressure drop characteristics of the bottom nozzle since the flow area through the grillage has not been altered.

Above the active fuel region of the core and below the top nozzle, the ZRFRA and stainless steel designs have slight elevation differences in upper spacer grids and fuel rod tops (see Figure 5-3). The axial positioning of the upper spacer grid for the ZRFRA design will have

no impact on the overall core pressure drop.
At the beginning-of-life (BOL) for the ZRFRA design, the gap between the top of the fuel rods and the bottom of the top nozzle is approximately 1.5 inches larger than the gap for the stainless steel design. The larger vertical gap in the ZRFRA design results in a slightly larger pressure drop of 2 percent.

Combining all the pressure drop effects from below and above the active fuel region, the ZRFRA design has a 3 percent larger core average pressure drop than the stainless steel design. This difference, which decreases as the Zircaloy fuel rods increase in length because of irradiation growth, is within the prediction uncertainty of pressure drop for the original design, therefore, does not represent a change.

The increase in the core average pressure drop for a full core of ZRFRA design fuel assemblies also results in an increase in the hydraulic lift force exerted on the fuel assemblies. The holddown springs on the ZRFRA design provide adequate holddown force margin for the fuel assembly under normal operating conditions and during the fourth reactor coolant pump startup conditions (presently at 465°F).

5.3. DNB Performance

The DNB performance of a fuel design is dependent on the fuel rod surface heat flux and the coolant conditions in the subchannel. In the case of the ZRFRA design, the fuel rods have the same fuel rod outer diameter as the fuel rods of the stainless steel design. However, the reduction of the fuel stack height from 120.5 inches for the stainless steel design to 118.575 inches for the ZRFRA design has increased the average heat flux by 2 percent. Thermal hydraulic analyses for the ZRFRA design will reflect the DNBR impact of the higher heat flux which is approximately 3 percent in DNBR.

The slightly higher core average pressure drop identified in Section 5.2 for a full core of the ZRFRA design will have an insignificant impact on the DNB performance of the design. Since the ZRFRA design employs the same spacer grids and fuel rod outer diameter as the stainless steel design, the local bundle and subchannel characteristics of thermal mixing, turbulence intensity, and lateral crossflow interchange will be the same for the two designs. PIE results of the LTAs indicate the magnitude of fuel rod bow for the ZRFRA is similar to the other BWFC Zircaloy clad fuel assembly designs. This similarity of in-reactor performance justifies the application of the conservative fuel rod bow prediction correlation for water channel closure presented in the B&W fuel rod bow topical report (Reference 10). The topical report concludes no DNBR reduction due to fuel rod bow need be considered in-reactor licensing. This conclusion is based on the following:

1) For fuel assemblies with burnups up to 24,000 MWd/mtU, the DNBR reduction

caused by fuel rod bow is less than 1%.

2) The power production capability of fuel assemblies diminishes with irradiation to the extent that fuel assemblies with burnups of 24,000 MWd/mtU or more cannot produce enough power to achieve design limit peaking values.

The 1% DNBR reduction attributed to rod bow for fuel with burnups up to 24,000 MWd/mtU is bounded by the fuel rod pitch variation allowance incorporated into the enthalpy rise engineering hot channel factor, $F_{\Delta H}^{N}$, for DNBR analyses.

5.3.1. Engineering Hot Channel Factors

Engineering hot channel factors are applied to predicted core power distributions to account for the effects of manufacturing variations and flow conditions. These factors are made up of statistically combined sub-factors which account for the influence of variations in parameters that affect subchannel coolant enthalpy rise and local heat flux.

5.3.1.1. Heat Flux Engineering Hot Channel Factor, F_Q^E

The heat flux engineering hot channel factor is used to evaluate the maximum linear heat generation rate in the core. This factor is determined by statistically combining manufacturing variations in fuel weight per unit length, enrichment, and fuel rod diameter. Using manufacturing tolerances, this factor has been conservatively determined to be 1.02 (Reference 15), for stainless steel and Zircaloy clad fuel, which has been approved by the NRC (Reference 16). $F_Q E$ is used to evaluate the peak linear heat generation rate and does not need to be considered in DNB evaluations. References 17 and 18 support the position that local heat flux spikes, such as that represented by $F_Q E$, have a negligibly small effect on the critical heat flux and therefore need not be considered in DNB analyses.

5.3.1.2. Enthalpy Rise Engineering Hot Channel Factor, $F_{\Delta H}^E$

The enthalpy rise hot channel factor accounts for the effects of variations in parameters that affect subchannel enthalpy rise. Items considered that contribute to this variation include:

1.0 Pin power, which is proportional to fuel stack weight and enrichment, rod diameter pitch and bowing:

The pin power sub-factor is a combination of manufacturing tolerances on stack weight and enrichment. The rod diameter, pitch and bowing variations are accounted for by determining a minimum subchannel flow area, based on fuel assembly specification tolerances, then calculating the pin power factor which

provides an equivalent DNBR effect. This factor is then combined statistically with the pin power sub-factor into the engineering hot channel factor. The resulting factor is 1.067.

2. Core inlet flow maldistribution:
   A pin power factor of 1.03 is applied to produce a DNBR effect equivalent to an inlet flow maldistribution.

3. Flow redistribution:
   Flow redistribution within the core results from the non-uniform radial power distribution. Flow is reduced in the hot subchannel because of increased flow resistance caused by local boiling. This effect is modeled directly in the core thermal-hydraulic analyses, therefore has no effect on the engineering hot channel factor.

4. Flow mixing:
   Flow mixing is accounted for directly in the subchannel thermal-hydraulic models, therefore has no effect on the engineering hot channel factor.

5.3.2 Densification Power Spikes

As the fuel undergoes irradiation in the reactor core, it experiences a phenomenon known as densification. This behavior of axial and radial shrinking plays a critical part in determining the fuel temperature of the fuel pellet since the fuel/clad gap is a major factor in temperature calculations. The radial densification mainly effects the fuel thermal performance, however, the axial densification plays a part in the nuclear behavior if unusual circumstances exist.

If a fuel pellet stack experiences densification, the height of fuel pellets shortens and allows the stack height to also shorten. If this occurs, the pellets would be expected to settle lower in the fuel rod. If by chance, a pellet or series of pellets wedge tight in the fuel rod, thus preventing the stack from settling, there could exist an axial gap below the wedged pellet(s).

A gap in the fuel stack would result in a reduction in the neutron absorption within the fuel rod. This will lead to an increase in the neutron flux on the adjacent fuel rods at the axial location of the gap. This increase in neutron flux would result in increased localized peaks. In order to account for this possibility, the current Haddam Neck Technical Specifications include a "Spike Penalty" that is applied to measured values of core power peaking factors when these values are compared to the Linear Heat Generation Rate (LHGR) limits. The basis for these limits is to provide assurance that the initial conditions assumed for the

LOCA are met.

The spike penalty, also known as a densification power spike factor, represents the power spike that could occur in surrounding fuel rods as the result of a densification-induced gap in a fuel column. This factor is typically calculated from a conservative set of assumptions, including the maximum predicted densification value, without consideration of thermal expansion or fuel pellet swelling effects.

References 19 and 20 concluded that the densification power spike penalty can be eliminated from LOCA analyses. This conclusion was based on transient sensitivity studies showing that radiant heat transfer to the cool cladding surrounding the inter-pellet gap would reduce peak cladding temperatures to levels lower than those that occur in fuel rod arrays with no inter-pellet gaps.

References 19 and 20 also concluded that the densification power spike penalty need not be considered in DNBR calculations on the basis that the heat flux spikes conservatively representative of fuel densification effects have a negligibly small affect on critical heat flux.

Additional support for the elimination of the densification power spike from further consideration is provided in Reference 21, in which axial gap data from three PWR fuel suppliers (including B&W) was utilized, with the conclusion that:

> "... modern, prepressurized fuel rods loaded with nondensifying UO_2 fuel pellets, are considered to be resistent to interpellet-gap formation and clad collapse. Therefore, the penalty for densification caused augmented power peaking should be removed from the analysis and licensing requirements of any reactor loaded exclusively with fuel rods of such modern design."

Since the fuel rods loaded in the Haddam Neck core (both stainless and Zircaloy clad) are "modern design" (95% theoretical density in prepressurized fuel rods), it is concluded that the use of densification power spikes is no longer necessary for either DNBR or LOCA considerations and that the spike factor in the current Technical Specifications can be deleted.

5.4. Fuel Rod Performance

The Zircaloy clad fuel rod performance as a function of burnup has been determined using the TACO2 code, Reference 3. Fuel pellet temperatures and fuel rod internal pressure predictions have been made with TACO2 using the standard methodology of Reference 3 to

establish the fuel melt limit, and to establish the fuel rod burnup at which the rod internal pressure is equal to the nominal coolant pressure.

5.5. Transition Cycles

The ZRFRA fuel design will be introduced into the Haddam Neck core in a series of three fuel reload batches. During the two transition cycles when the ZRFRA and stainless steel designs will operate together in the core, the hydraulic effects of two adjacent fuel designs are of interest. These effects can be categorized as follows:

a) hydraulic compatibility effects, and
b) DNBR effects.

The hydraulic differences between full cores of the Zircaloy and stainless steel designs have been discussed in Section 5.2. When the two designs operate adjacent to one another, the impact of the hydraulic differences become more significant. The differences identified in Section 5.2 are:

a) The height of the ZRFRA bottom nozzle legs is less than that of the stainless steel design (see Figure 5-1).
b) The ZRFRA top and bottom spacer grids are slightly more "inboard" to the fuel assembly than for the stainless steel design (see Figures 5-2 and 5-3), resulting in slighdy different axial positions for the spacer grids.
c) The vertical gap between the top of the fuel rods and the bottom of the top nozzle is larger for the Zircaloy design than the stainless steel design (see Figure 5-3).

The difference in height of the bottom nozzle legs for the two fuel assembly designs will have no impact on the inlet flowrates for the respective fuel types. The axial elevations of the end spacer grids of the Zircaloy design are set such that adequate grid-to-grid matchup is maintained to avert a flow sweeping effect around the end spacer grids of an adjacent stainless steel clad fuel assembly.

Thermal hydraulic analyses have shown that the introduction of the ZRFRA design into the Haddam Neck core will have a small impact on the core DNBR performance of the ZRFRA design. Since the ZRFRA design has a slightly higher pressure drop than the resident stainless steel design, the bundle flowrates through the ZRFRA assemblies will be smaller than the flowrates through the stainless steel clad assemblies during the transition cycles. This flowrate reduction reduces the predicted DNBR for the ZRFRA design by less than 1 percent in DNBR during the first transition cycle relative to the predicted DNBR for a full core of ZRFRA assemblies. This DNBR transition penalty decreases for each subsequent transition cycle and will be addressed on a cycle-by-cycle basis.

Figure 5-1. Zircaloy Clad and Stainless Steel Clad
Bottom Nozzle

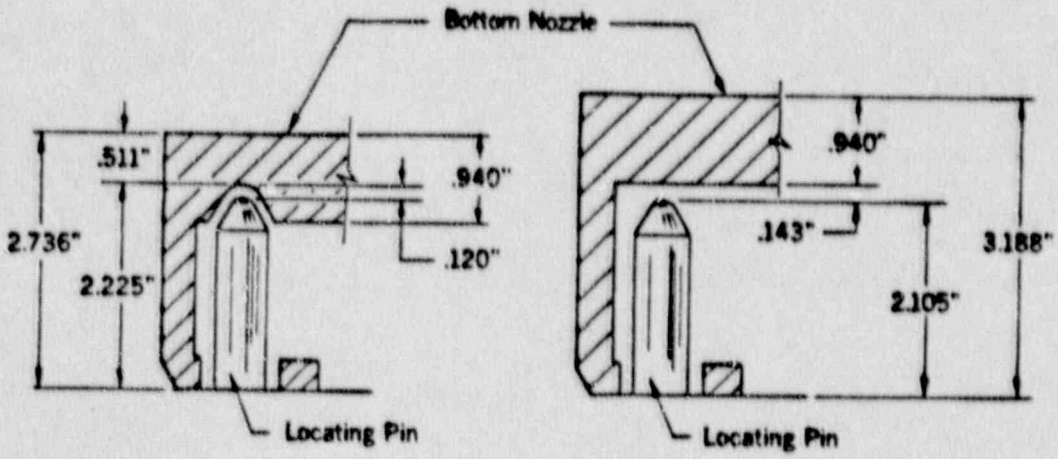

Figure 5-2. Zircaloy Clad and Stainless Steel Clad

Bottom Spacer Grid Interface

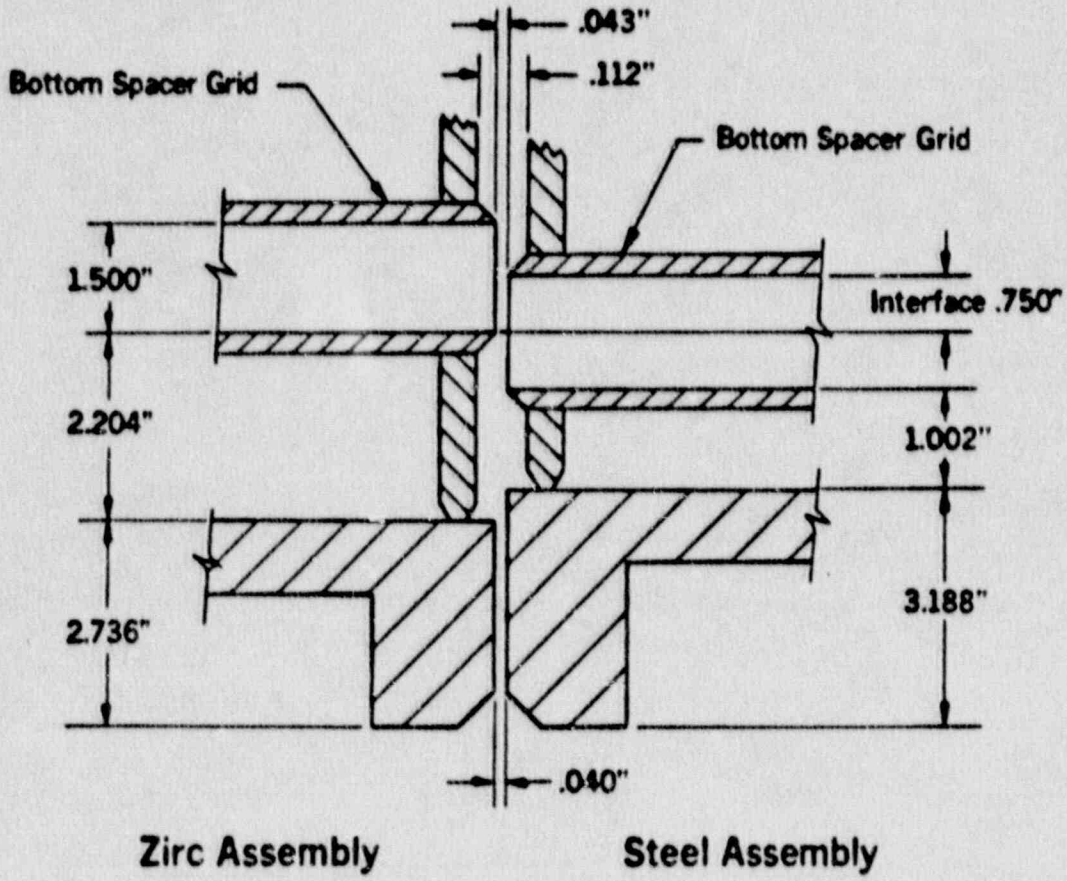

Figure 5-3. Zircaloy Clad and Stainless Steel Clad

Top Spacer Grid Interface

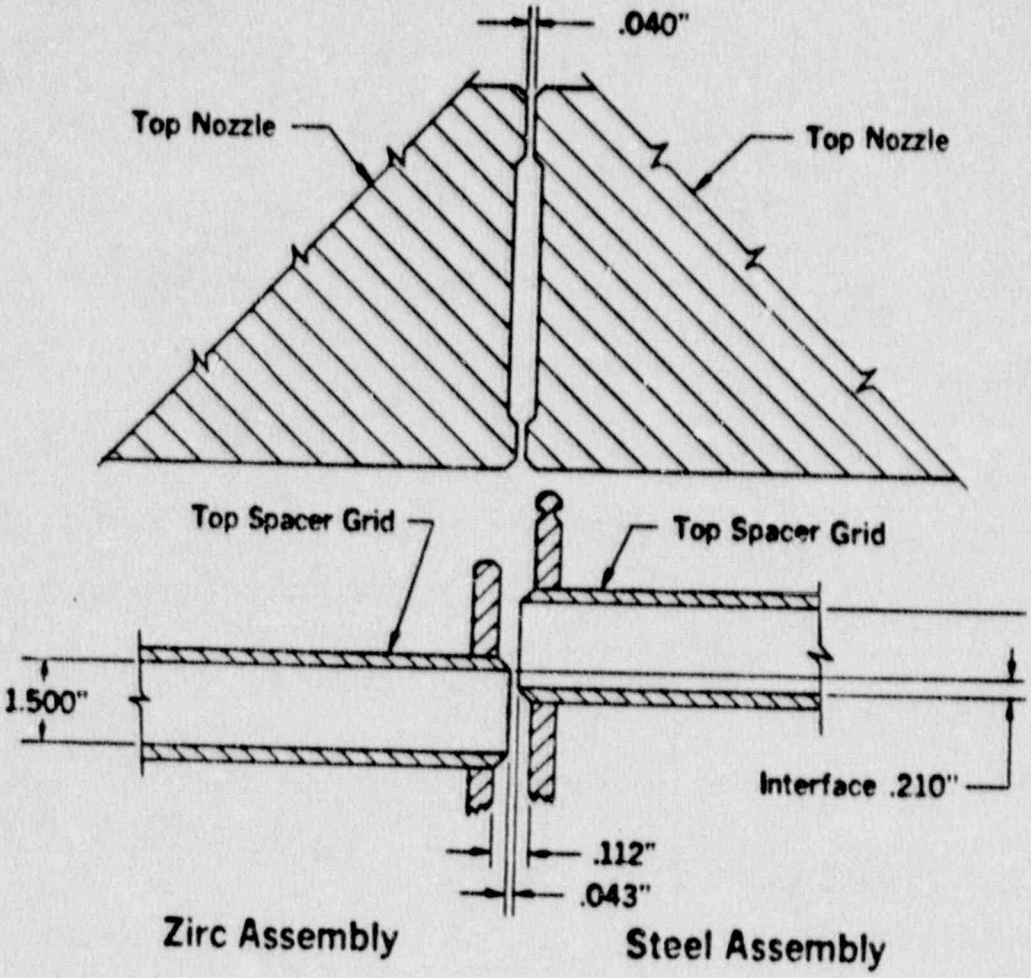

6.0 CONCLUSIONS

The mechanical design of the Zircaloy clad fuel assembly has been shown to meet the design goals provided in Section 2.0. The mechanical design features were provided in Section 3.0, and compared with the stainless steel and LTA designs. This comparison shows that the number of non-cladding design changes was minimized to assure compatibility with the stainless steel clad fuel assembly. The mechanical design analyses provided in Section 4.0 have been performed using approved B&W standard design methodologies, and all acceptance criteria were met. The thermal hydraulic evaluations provided in Section 5.0 demonstrate the compatibility with the stainless steel clad design. The slight increase in pressure drop has a negligible impact on the minimum DNBR.

Based on the results of these evaluations and the performance of the four Lead Test Assemblies, the Zircaloy clad fuel assembly design can safely operate in the Haddam Neck core up to a maximum fuel assembly burnup of 50,000 MWd/mtU.

7.0 REFERENCES

1. Standard Review Plan, Section 4.2, NUREG-0800, Rev 2, U.S. Nuclear Regulatory Commission, July 1981.

2. ASME Code Section III, "Nuclear Power Plant Components," 1983 Edition.

3. TACO2 Fuel Pin Performance Analysis, BAW-10141P-A, Rev. 1, Babcock and Wilcox, Lynchburg, Virginia, June 1983.

4. W. J. O'Donnell and B. F. Langer,"Fatigue Design Basis for Zircaloy Components." Nuclear Science and Engineering, Volume 20, pages 1-12.

5. Program to Determine In-Reactor Performance of B&W Fuels--Cladding Creep Collapse--BAW-10084P-A, Rev. 2, October 1978.

6. J. H. Taylor to C. O. Thomas, "Creep Collapse Analysis of B&W Fuel," JHT/86-011A, January 31, 1986.

7. D. M. Crutchfield to J. H. Taylor, "Acceptance for Referencing of a Special Licensing Report," December 5, 1986.

8. Extended-Burnup Evaluation, BAW-10153P-A, April 1986.

9. RDD:88:5431-02:01, PIE Results on Mark BZ Zircaloy Grids After Three Cycles. J. T. Mayer and T. D. Pyecha, December 10, 1987.

10. Fuel Rod Bowing in Babcock & Wilcox Fuel Designs, BAW-10147P-A, Rev. 1, Babcock & Wilcox , Lynchburg, Virginia , May 1983.

11. Mark-C Fuel Assembly LOCA-Seismic Analyses, BAW-10133P, Rev-1, Babcock & Wilcox, Lynchburg, Virginia, June, 1986.

12. Babcock & Wilcox - NPGD Water Chemistry Manual Duke Type Plants, BAW-1385, Revision 4, April 1985.

13. EPRI NP-5960-SR. PWR Primary Water Chemistry Guidelines: Revision 1, August 1988.

14. LYNX1: Reactor Fuel Thermal Hydraulic Analysis Code, BAW-10129-A, Babcock & Wilcox, Lynchburg, Virginia, July, 1985.

15. J. F. Opeka (CYAPCO) to C. I. Grimes (USNRC) "Additional Information for Proposed Revision to Technical Specifications, Cycle 14 Reload," February 6, 1986.

16. F. M. Akstulewicz to J. F. Opeka (CYAPCO), "Cycle 14 Reload Technical Specifications," April 14, 1986.

17. K. E. Suhrke (B&W) to S. A. Varga (NRC), December 6, 1976.

18. S. A. Varga to J. H. Taylor (B&W), Subject; Update of BAW-10055, "Fuel Densification Report," December 5, 1977.

19. Letter, K. E. Suhrke (B&W) to S. A. Varga (NRC), December 6, 1976.

20. Letter, S. A. Varga (NRC) to J. H. Taylor (B&W), Update of BAW-10055, "Fuel Densification Report", December 5, 1977.

21. EPRI Report NP-3966-CCM, "CEPAN Method of Analyzing Creep Collapse of Oval Cladding, Volume 5: Evaluation of Interpellet Gap Formation and Clad Collapse in Modern PWR Fuel Rods", Combustion Engineering, Inc., April 1985.